Adsorption of Dimethyl Methylphosphonate on Self-Assembled Alkanethiolate Monolayers

Lars Bertilsson, Karin Potje-Kamloth, and Hans-Dieter Liess

Universität der Bundeswehr München, Fakultät für Elektrotechnik, Institut für Physik, Werner-Heisenberg-Weg 39, D-85577 Neubiberg, Germany

Isak Engquist and Bo Liedberg*

Molecular Films and Surface Analysis Group, Laboratory of Applied Physics, Linköping University, S-581 83 Linköping, Sweden

Received: October 1, 1997; In Final Form: December 1, 1997

The adsorption of dimethyl methylphosphonate (DMMP), a model molecule for sarin, on three different organic interfaces, prepared by solution self-assembly of alkanethiols on gold, was followed by a surface acoustic wave mass sensor and infrared reflection−absorption spectroscopy at room temperature. The surfaces, characterized by the following tail groups (−OH, $-CH_3$, −COOH), show both quantitative and qualitative differences concerning the interaction with DMMP, the acid surface giving rise to the strongest adsorption. Results obtained in UHV, at low temperatures using infrared spectroscopy and temperature-programmed desorption, support this observation and give complementary information about the nature of the interaction. The hydrogen-bond-accepting properties of the P═O part of DMMP and its impact on the design of sensing interfaces based on hydrogen bonding, as well as the use of self-assembled monolayers to study molecular interactions, are discussed.

Introduction

Sensors for gases and vapors based on selective absorption all depend on molecular interactions. Adsorption/absorption of an analyte in for instance a polymer layer may involve different types of interactions, and the characteristic behavior of the sensor, concerning sensitivity and selectivity, relies upon the strength of these interactions. The hydrogen bond is one type of molecular interaction that can increase the partition coefficient of such a layer enough to allow detection of gases capable of accepting or donating protons to establish hydrogen bonds. On the other hand, it is weak enough to ensure reasonable time constants for dissociation and desorption.

Dimethyl methylphosphonate is commonly used as a model molecule for the highly toxic sarin during the development of sensors and the study of catalytic decomposition of organophosphonates.[1] In this study, we are examining its interaction with three well-characterized organic surfaces prepared by solution self-assembly of ω-substituted alkanethiols SH−$(CH_2)_m$−X on gold surfaces. The surfaces formed in this way are well-characterized and known to form ordered monomolecular assemblies, with interfacial properties determined primarily by the tail group X.[2] Thus, our system shows similarities with solid-state surfaces used for controlled adsorption experiments in pure surface physics. In this way, basic molecular interactions normally obscured by the bulk properties of organic polymers can be resolved. Even though there will be a need of thicker polymer films in a real sensor, in order to collect the analyte and reach reasonable sensitivity and selectivity levels, it is felt that this type of examination can contribute to the understanding of the basic mechanisms and thus to the development of improved protocols for design of artificial sensing layers.

* Corresponding author. E-mail: bol@ifm.liu.se.

The surface acoustic wave (SAW) sensor, used here as a gravimetric sensor, is extremely sensitive to changes in a number of physical parameters. Mostly, its response is considered to be exclusively due to changes in mass on the surface between the interdigital transducers (IDTs) used to convert the electrical signal into a acoustic surface wave and vice versa. With this assumption, the used device has a theoretical detection limit of less than 1 % of a DMMP monolayer. It has been shown, however, that changes of the viscoelastic properties of films also can influence the result[3] and that this becomes a serious problem when the sensing layer is thick as compared to the wavelength of the acoustic wave. Compared to the thickness of the self-assembled monolayers (SAMs), the wavelength of the used device, 20 μm, is 4 orders of magnitude larger, and changes in the film stiffness would have to be of considerable magnitude to cause a relevant contribution to the response. There are, however, examples in the literature[4] which indicate that the viscoelastic properties can contribute to the overall sensing signal.

In earlier work, we have shown that DMMP interacts with hydroxyl groups through hydrogen bonding where the P═O group acts as hydrogen-bond acceptor. The adsorption experiments were carried out using infrared reflection−absorption spectroscopy (IRAS) and temperature-programmed desorption (TPD) under UHV conditions.[5] We also used a SAW sensor setup and IRAS under realistic conditions to gain detailed information about the interactions involved.[6] In this paper we extend the efforts on using SAMs as sensing layers by introducing a new model surface, which is expected to display a strong hydrogen bond with DMMP, the −COOH surface, and we analyze the variation in hydrogen-bond pattern for the different interfaces at DMMP coverages of less than one monolayer.

S1089-5647(97)03215-X CCC: $15.00
Published on Web 01/23/1998

Experimental Section

Surface Monolayer Preparation. The surfaces used for IRAS (infrared reflection−absorption spectroscopy) experiments (10 Å Cr and 2000 Å Au sputter coated on 20 × 20 mm^2 glass substrates at a background pressure of $<10^{-6}$ Torr) and for TPD (25 Å Ti and 2000 Å Au electron beam evaporated on 20 × 20 mm^2 Si substrates at a background pressure of $<10^{-9}$ Torr), as well as the SAW devices (see below), were cleaned in piranha solution (H_2O_2(30%):H_2SO_4(98%), 1:3 by volume; *caution*: reacts violently with organic material and should not be stored!) for 1 min, rinsed with copious amounts of water (Millipore) and with ethanol, and introduced in ethanol solutions (Bundesmonopolverwaltung für Branntwein Sorte 430, 96%) of thiols with a total concentration of 2 mM. $SH-(CH_2)_{15}-CH_3$ (Aldrich, 92%) was vacuum distilled (8 Torr, 470 K, Ar); $SH-(CH_2)_{16}-OH$ and $SH-(CH_2)_{15}-COOH$ (a generous gifts by Dr. Löfås, BIACORE AB, Uppsala, Sweden) were used as received. After adsorption overnight, the surfaces were rinsed in ethanol, cleaned in ultrasonic ethanol bath 10 min, dried in a stream of N_2, and introduced into the gas cells. The −COOH-terminated SAM was shortly rinsed in HCl solution (pH = 3.5) before introduction into the measurement cells, to ensure a protonated acid.

SAW Experiment. A SAW delay line working at a frequency of $f_0 = 149$ MHz was designed by us and produced on ST-quartz in the Paul Drude Institut für Festkörperphysik, Berlin. The IDTs and the delay line between the IDTs consist of 130 nm Au on Cr. Structures for direct surface temperature measurements are added on the surface. All experiments were made at room temperature, and temperature drift was compensated for by simultaneous temperature measurements. The device was used in the oscillator configuration with homemade electronic circuits, and the short-term noise was <2 Hz. The theoretical sensitivity is given by eq 1, where f is the frequency, K is a geometrical constant equal to the fraction of the IDT center-to-center distance affected by the adsorption (=1, see Discussion Section), $c_m = 1.7$ cm^2 g^{-1} MHz^{-1} (ref 7), and Δm is the change in surface mass (g cm^{-2})

$$\Delta f/f_0 = -Kf_0c_m\Delta m \quad (1)$$

The sensitivity is 27 pg cm^{-2} Hz^{-1}, which results in a practical detection limit of approximately 100 pg cm^{-2}. Saturated DMMP (dimethyl methylphosphonate, Fluka, >97%) vapor was produced using a bubbler. The carrier gas was of high purity N_2 (Linde, 5.0), and dilution was performed using mass flow controllers (Whiga GmbH). Flow rates of 50−500 cm^3 min^{-1} were used. The change of flow rates for dilution purposes was found not to induce any unwanted effects in the measurements.

IRAS. Vibrational absorption spectra were measured with a Bruker IFS66 FTIR spectrometer purged with dry air. Infrared reflection−absorption spectra were collected using a home-built gas cell, allowing measurements at an angle of incidence of 83°. The cell has a volume of 1.5 cm^3 and a path length of 27 mm and is closed by CaF_2 windows. Before entering the gas cell, the light is polarized by a KRS-5 metal grid polarizer (Graseby Specac, 0.12 μm Al strips), allowing measurements with light polarized either perpendicular (s-) or parallel (p-) to the plane of incidence. Normally 2000 scans (10 min) were collected at a resolution of 2 cm^{-1} (zero filling factor 2) using a liquid nitrogen cooled MCT detector. Reference spectra were collected in N_2 (surface without adsorbed DMMP molecules). As the molecular adsorption studied is of reversible character at room temperature, the gas-phase molecules present in the measurement cell at equilibrium will contribute to the infrared intensities and thus overlap with the peaks due to the adsorbed molecules. It is, however, possible to compensate for the gas-phase contribution, and the spectra shown below are all obtained in the following way. A spectrum of the adsorbed DMMP was collected during the DMMP pulse (R), using p-polarized light, and divided by a spectrum collected before the pulse but in the same carrier gas (R_0). The resulting spectrum contains information originating from the adsorbed as well as the gas-phase DMMP and also from changes in the SAM caused by the adsorption of DMMP. The spectra were then compensated for the gas-phase absorption by subtracting a pure gas-phase spectrum of DMMP. A useful gas-phase spectrum can be obtained with the same gas cell using s-polarized light (not surface sensitive[10]). In this way only the adsorbed DMMP molecules, and the changes that are introduced in the SAM due to the adsorbed molecules, can be seen.

Liquid sample measurements were performed using a liquid cell with CaF_2 windows and 6 μm Mylar spacers; 10 scans were collected at a resolution of 2 cm^{-1} using decanol (EGA-Chemie, 99%), octanoic acid (Merck, >99%), and hexadecane (Aldrich, >99%).

UHV Measurements. The UHV chamber used[8] and the experimental details[5] have been described previously. Infrared reflection−absorption spectra were collected with an attached Bruker IFS 113v FTIR spectrometer, equipped with a liquid nitrogen cooled MCT detector. Measurements were performed at an angle of incidence of 85°, by averaging 500 scans at a resolution of 2 cm^{-1} (zero filling factor 2).

The combined IRAS and TPD experiments were made as follows: The sample surface was cooled to, and maintained at, 100 K, and an IRAS spectrum was collected (R_0). After deposition, a new spectrum was collected (R) and divided by R_0. In this way, only absorption peaks due to the adsorbed molecules or due to the changes that are introduced in the self-assembled monolayer by the adsorbed molecules are seen. Finally, temperature-programmed desorption was made, using a linear heating ramp of 0.33 K s^{-1} and monitoring several masses with a positive ion counting mass spectrometer (Hiden HAL 3F/301). Two different doses, expressed as langmuirs (1L = 10^{-6} Torr s), of DMMP were examined in order to evaluate the coverage dependence. The given doses are corrected for the difference in pressure between the pressure sensor and the surface (due to the deposition capillary). The correction is valid for D_2O, and thus the DMMP doses might have a systematic error.

Contact Angle Measurements. The contact angle of water on the SAW surfaces was measured with the sessile drop technique using a modified microscope. This was used as quality control of the surface modifications.

Results and Discussion

Self-Assembled Alkanethiolate Monolayers. The three different self-assembled monolayers (SAMs) used throughout this study were prepared from ethanolic solution (2 mM) of $SH-(CH_2)_{16}-OH$, $SH-(CH_2)_{15}-CH_3$, and $SH-(CH_2)_{15}-COOH$ (in the following called the −OH, $-CH_3$, and −COOH surface, respectively). The self-assembly process of these molecules is well-documented, and we refer to the extended literature on this topic.[2] As a quality control of the assembly process, the position of the CH_2 backbone modes can be used, and in Table 1 we have listed the peak positions in the C−H stretching region. The positions of the CH_2 ν_{as} at 2919 cm^{-1} and ν_s at 2850 cm^{-1} modes are consistent with the all-trans configuration expected for well-ordered layers.[2a]

TABLE 1: Infrared Absorptions of the Self-Assembled Monolayers Used[a]

surface	$\nu_{as}(CH_2)$	$\nu_s(CH_2)$	$\nu_{as}(CH_3)$	$\nu_s(CH_3)$	CH_2*
−OH	2919	2850			2878
−COOH	2919	2851			
$-CH_3$	2918	2850	2965	2877	

[a] Shown are the main absorptions in the C−H stretch region. The CH_2* position is due to the CH_2 group closest to the −OH.

In the case of the monolayers formed on SAW delay lines, the dimensions of the Au surface between the IDTs (2×4 mm^2) exclude direct IRAS measurements. However, the surfaces were prepared and pretreated in the same way as those used in the IRAS experiments, and comparison of contact angles showed no discrepancy.

Adsorption Isotherms of DMMP at Room Temperature. The mass changes due to adsorption of DMMP on the three different SAMs were followed by the SAW sensor. With this method the change in surface mass is recorded as a change in oscillator circuit frequency upon introduction of DMMP in the nitrogen carrier gas stream. Equilibrium was reached after a few minutes, and between each pulse the system was purged with N_2. The frequency shift can be converted into a surface coverage if the mass of one monolayer and the mass sensitivity of the SAW device are known (see Experimental Section for details). However, when interpreting the quantitative results from coated SAW sensors, the geometry of the device must be carefully considered. The distance traveled by the surface acoustic wave is not totally covered with the thin gold film and thus with the SAM. This is due to the interdigital transducers (IDTs) needed to transmit and receive the acoustic waves. The uncovered part consists of naked quartz, which is highly hydrated due to the piranha pretreatment. If the adsorption on this part of the delay line is considered, we might need to correct the results. Assuming that 10% of the IDT center-to-center distance of one delay line that is naked quartz has similar adsorption characteristics as an −OH surface, the frequency shift is expected to be of the same magnitude as the one measured for the $-CH_3$ surface. Thus, the isotherms obtained for weakly interacting surfaces, as the hydrophobic $-CH_3$ surface, should be corrected for this additional adsorption before any conclusions can be drawn. The two isotherms labeled with $-CH_3$, in Figure 1, represent the results with (▼) and without (●) this compensation, and in the forthcoming discussion we refer to the compensated isotherm. The contribution to the measured frequency changes due to adsorption on the naked quartz has consequences also in the case of the hydrophilic SAMs used in this study. As a first-order approximation we assume that the adsorption is uniform on the whole delay line. Thus, we do not distinguish between adsorption on SiOH- and OH/COOH-terminated organic surfaces. This means that the geometrical factor, *K*, describing the fraction of the total distance between the IDTs that contributes to the sensing signal, should be set to one in the standard mass sensitivity formula eq 1 for the used type of SAW device. In doing so, a frequency decrease of 2.5 kHz for one DMMP monolayer can be calculated, and this value was used to obtain the coverages. The uncertainty of the correction, together with the fact that surface roughness is not considered in the calculation, suggests that the calculated equilibrium surface coverages should not be taken absolute but rather as a convenient way to compare the three surfaces.

The dependence on the DMMP concentration was followed in a concentration range giving rise to coverages below one monolayer. Typical results for the three different surfaces are shown as isotherms in Figure 1, where the solid lines are fits

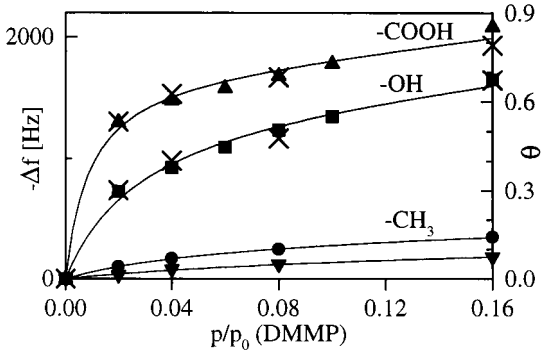

Figure 1. The DMMP surface coverage as a function of gas-phase concentration (p/p_0). The isotherms were measured using a SAW sensor covered by SAM with the tail groups −COOH (▲) and −OH (■), and the coverage, θ (right), was calculated from the frequency shift, Δf (left), as described in the text. The lines are fits using BET theory. For the $-CH_3$ surface original (●) and corrected (▼) results are shown. The correction takes into account the adsorption on the parts of the delay line not covered by the SAM, and details of the correction are described in the text. Also shown (×) are the results from scaled integrated intensity of IRAS peaks at ∼3300−3400 cm^{-1} (OH band).

using the BET theory,[9] eq 2. The total number of adsorbed molecules, n_a, is in eq 2 expressed as a function of the number of adsorption sites in the strongly interacting monolayer, n_0, a constant, *c*, the pressure, *p*, and the relative pressure *z* ($z = p/p_0$, where p_0, is the saturated vapor pressure).

$$n_a = \frac{n_0 cz}{(1 - z)(1 + (c - 1)z)} \tag{2}$$

The constant, *c*, is normally defined as

$$c = \exp[(\Delta H_a - \Delta H_l)/RT] \tag{3}$$

where ΔH_a is the enthalpy of adsorption corresponding to the n_0 surface sites and ΔH_l the enthalpy of adsorption in the following layers, mostly taken to be equal to the heat of liquefaction, and we will return to this later. Both n_a and n_0 can be expressed as coverages (θ and θ_0, respectively) by considering the number of DMMP molecules in one monolayer.

There is a clear increase of adsorbed DMMP in going from the $-CH_3$ surface via the −OH surface to the −COOH surface. This is best illustrated at the lowest concentration used, $p/p_0 = 0.02$ (26 ppm). At $p/p_0 = 0.02$ the fitted isotherms give coverages, θ, of <0.05, 0.3, and 0.5 monolayer (ML), respectively. The number of surface sites, n_0, obtained from the BET curves corresponds to θ_0 values of 0.6 ML for the −OH surface and slightly higher, ∼0.7 ML, for the −COOH surface while the $-CH_3$ surface shows a much lower value of approximately 0.1 ML. This indicates that only a portion of the surface groups are contributing to the stronger interaction, the rest acting as moderately strong sites. The property of interest for a sensor based on this type of interaction is the sensitivity to changes in concentration at very low levels, given by the initial slope of the isotherms, $d\theta/dp$. This can be used to compare the surfaces and gives a change in coverage, θ, of 0.7% ppm^{-1} for the $-CH_3$ surface, 3% ppm^{-1} for the −OH surface, and 9% ppm^{-1} for the −COOH surface. However, the slope of the BET isotherm only gives an estimate of the sensitivity. The reason for this uncertainty is that the enthalpy of adsorption is assumed to be independent of surface coverage in the first monolayer in the BET theory; i.e., all surface sites are equal. In reality, the enthalpy of adsorption probably shows a coverage dependence. For the −OH surface, the IRAS results suggest an increased

TABLE 2: Infrared Peak Positions for DMMP (in cm^{-1})[a]

vibration	gas phase	liquid phase	surface adsorbed
ν_a CH_3	3014	2995	3010
ν_a CH_3	2962	2956	2962
ν_s CH_3	2859	2852	2858
δ_a P-CH_3	1471	1466	1467
δ_s O-CH_3	1423	1421	
δ_s P-CH_3	1315	1314	1315
ν P═O	1276	1245	1260−1180
ρ (O)CH_3	1188	1186	1188
ν_a P-O-C and/or δ_a P-O-C	1075/1050	1065/1038	1070/1044

[a] Vibrational assignments are taken from refs 14, 16, 21, and 22.

enthalpy of interaction at low coverages. Thus, the slope obtained by the BET theory may underestimate the sensitivity of this particular surface. We will return to this issue in the discussion below. With the uncertainty of this evaluation in mind, an estimation of the DMMP sensitivity of the used device with an −COOH monolayer indicates a detection limit below 100 ppb in N_2.

IRAS of the Adsorbed Molecules. Infrared reflection−absorption spectroscopy can be used to study the adsorption down to the submonolayer range. By analyzing changes in the spectral signature, conclusions can be drawn about the nature and strength of the molecular interaction involved, and relative coverages can be calculated from integrated peak intensities. The main features are the bands due to ν(P═O) and ν(PO−C), and in Table 2 the peak positions of DMMP are shown together with the vibrational assignments. With the used gas-phase compensation method (see Experimental Section), a small quantitative error could be introduced as the contribution from DMMP adsorbed with the P═O groups pointing out from the surface (free) will be subtracted. However, the importance of this is minor in the following discussion, due to the fact that the P═O part of DMMP is very prone to interact which will cause the peak position to shift. Earlier adsorption experiments[1e] have shown that the shift due to interaction can be as large as ∼100 cm^{-1}. It is also worth emphasizing that with the described procedure the SAM will not appear in the resulting spectra; only changes in the SAM structure will show up as negative or positive peaks.

DMMP−OH Interaction. By increasing the DMMP concentration up to where an equilibrium coverage close to 0.7 monolayer is reached, as measured by the SAW device, the intensity of all DMMP bands increases. If the IR peaks are integrated and used to quantify the adsorbed DMMP (not shown), isotherms of the same shape as the BET fit of the SAW response (Figure 1), are obtained. There are also some coverage-dependent spectral changes, the most pronounced ones being the shift of the O−H and P═O peaks (Figure 2, A and B).

At the lowest coverage ($p/p_0 = 0.02$) the P═O peak is found at 1235 cm^{-1} with a shoulder at ∼1212 cm^{-1}. If this spectrum is subtracted from the higher concentration spectra, the difference spectra show the structural progression in the outermost portion of the DMMP layer (lower panel of Figure 2B). In Table 3 the position of the main P═O peak of the DMMP added at different coverages displays a successive increase up to 1242 cm^{-1}. At the highest coverages a shoulder at ∼1260 cm^{-1} is also showing up. In the high wavenumber range, the main absorption is a broad peak at 3200−3550 cm^{-1} (Figure 2A). This is the position where hydrogen-bonded −OH modes are normally found, and the peak originates from changes in the hydrogen-bonding pattern of the surface −OH groups.[5] The

TABLE 3: Infrared P═O Peak Position of DMMP Adsorbed on an −OH Surface at Different Coverages

θ	ν(P═O)(cm^{-1})	θ	ν(P═O)(cm^{-1})
≪0.3	1212	0.4−0.5	1241
∼0.3	1235	0.5−0.7	1242 (1260)
0.3−0.4	1239		

coverage dependence of this band shows a clear increase in intensity, and the integrated peak intensity follows nicely the shape of the SAW isotherms (Figure 1). There is also a change in line shape as the concentration increases. At the lowest coverage the OH band appears at ∼3350 cm^{-1}, and with increasing coverage it shifts to ∼3450 cm^{-1}. The positive peaks at 2962 and 2858 cm^{-1} are due to the CH_3 modes of DMMP.

The DMMP adsorption results in the formation of hydrogen bonds between P═O and surface hydroxyls (O−H···P═O). It is known that the formation of hydrogen bonds increases the intensity of the infrared absorption substantially. As there are reasons to believe that the surface already consists of chains of laterally hydrogen-bonded hydroxyl groups,[11,12] hydrogen bonding itself can hardly be the only reason for the observed intensity increase. Another, perhaps more plausible, explanation is that a reorientation of the hydroxyl groups occurs upon adsorption, leading to a more favorable perpendicular orientation of the OH bond with respect to the surface. Thus, the increase in peak intensity is most likely due to the surface selection rule.[10] The lateral chains of hydrogen-bonded hydroxyls, however, could be the reason for the difference in strength found at different coverages. It is known that the strength of the hydrogen bonds increases due to "cooperative effects" in hydrogen-bonding networks.[13] It is also known that polymeric structures increase the strength of hydrogen bonds in alcohols.[14] If we assume that the adsorbed DMMP interacts with an OH at one end of such a chain, the strength of this interaction will be dependent on the length of that particular chain. At low coverage only a small amount of chains are interrupted by the adsorbed DMMP, and the average chain length is large, while at higher coverage the average chain length will decrease, and finally at a full monolayer one DMMP is left with only ∼1.5 OH. The corresponding −OH stretch vibration in polymeric structures is found at 3324−3347 cm^{-1} (strong hydrogen bonding), and for dimeric hydrogen bonds the absorption is found in the range 3550−3470 cm^{-1} (weak hydrogen bonding). This can be seen in results from liquid cell measurements where DMMP was allowed to interact with decanol in hexadecane (HD) (Figure 2, C and D). Pure decanol has a band at 3330 cm^{-1} due to chains of hydrogen-bonded OH and no bands in the 1230 cm^{-1} range. Upon adding a small amount of DMMP, the P═O peak (originally found at ∼1260 cm^{-1} in HD) shifts to 1237 cm^{-1} and the OH band shifts to 3440 cm^{-1}, with a shoulder still at 3330 cm^{-1}, indicating that breaking of the polymeric (lateral) OH···OH chains occurs. A further increase in the amount of DMMP shifts the P═O peak to 1241 cm^{-1}, and the low wavenumber shoulder near 3330 cm^{-1} on the OH band disappears. With this in mind, it is plausible that DMMP, at low coverage, interacts with the surface through hydrogen bonds with −OH groups that are involved in hydrogen-bonded polymeric chains (OH at ∼3350 cm^{-1} and P═O at ∼1235 cm^{-1}) and that at higher coverage the average chain length decreases (OH at ∼3450 cm^{-1} and P═O at 1241 cm^{-1}). Figure 3 shows a schematic view of the hydrogen-bonded surface hydroxyls and the effect of DMMP adsorption at different coverages.

The shoulder at approximately 1212 cm^{-1} for the lowest concentration originates from a stronger interaction. This might be due to adsorption at sites where occasionally more idealized

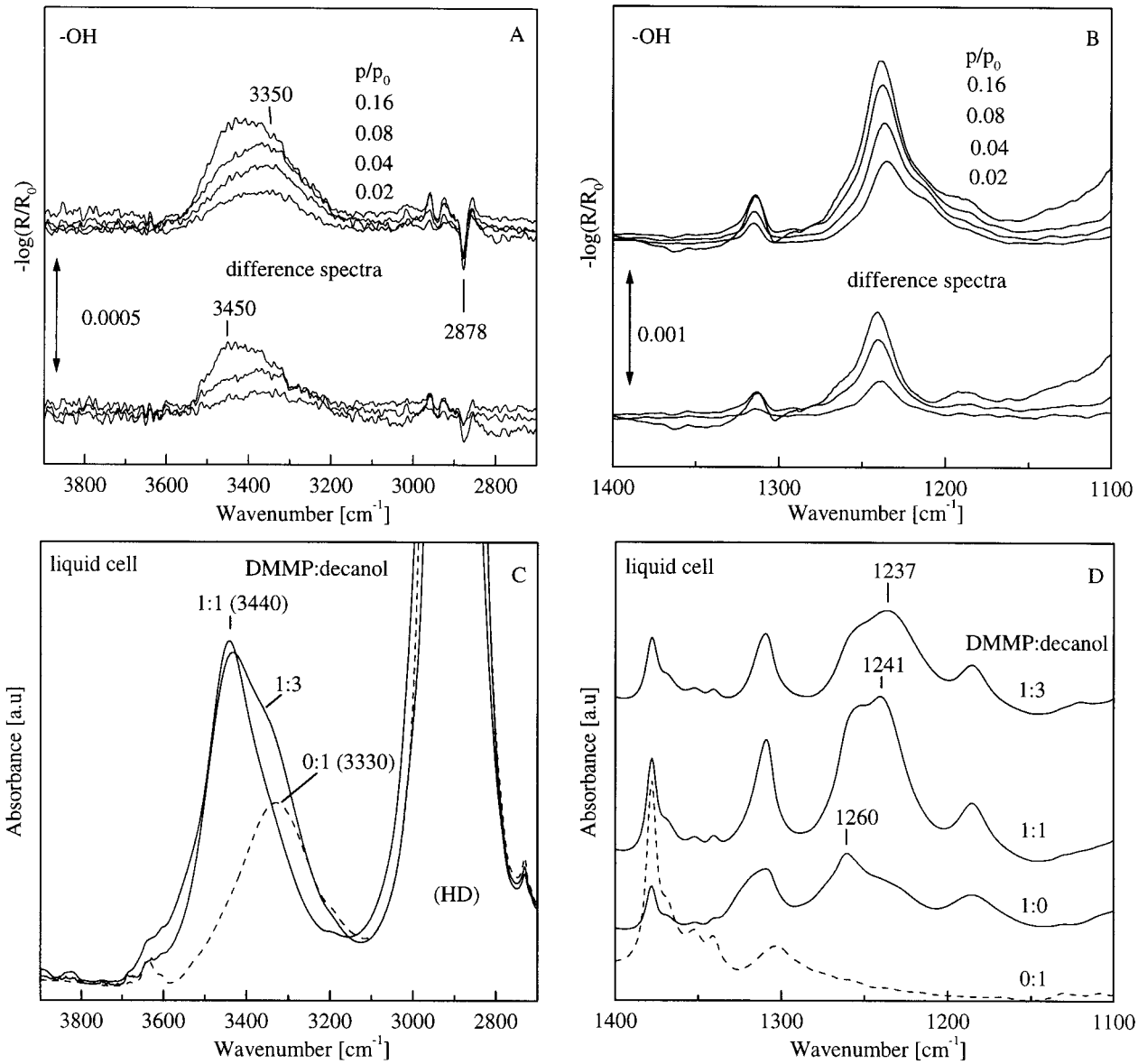

Figure 2. IRAS spectra of DMMP adsorbed on the −OH surface shown in the high wavenumber range (A) and the low wavenumber range (B). The relative concentrations of DMMP are indicated, and the difference spectra are obtained by subtracting the $p/p_0 = 0.02$ spectrum from the higher concentration ones. Liquid cell measurements of DMMP interacting with decanol in excess hexadecane as solvent are shown in the high wavenumber range (C) and the low wavenumber range (D), with the molar ratios indicated in the figures.

interaction can be allowed, i.e., hydrogen bonds involving both lone pair orbitals of the P═O oxygen.[5] This could be a statistical event due to thermal fluctuations in the outermost parts of the methylene chains in the SAM, but adsorption at defects, grain boundaries, or domain borders cannot be excluded as potentially important hydrogen-bonding sites.

The present room-temperature results agree well with our previous UHV observations at low temperatures,[5] supporting the conclusion that the strength of the interaction can be measured by shifts in peak positions of the groups involved in the hydrogen bonding. Furthermore, the large variation in the P═O and OH modes with exposure suggests that the enthalpy of adsorption is coverage-dependent, and the corresponding values obtained by the BET fit should be regarded as a first-order approximation.

DMMP−COOH Interaction. Upon increasing the DMMP concentration from zero to where an equilibrium coverage of ∼0.8 ML ($p/p_0 = 0.16$) was found by the SAW device, there is an increase in the intensity of the DMMP bands (Figure 4, A and B). Above $p/p_0 = 0.04$ the changes are smaller in correspondence with the SAW isotherms (Figure 1). Thus, isotherms of the same shape as for the SAW results are obtained if the infrared peaks are integrated (not shown). Higher coverage leads to a slight increase in intensity on the high wavenumber side of the P═O peak, indicating that the interaction is weaker. Compared to the −OH surface, the P═O peak is shifted toward lower wavenumbers with the main peak at 1220 cm^{-1} and a shoulder at ∼1210 cm^{-1} (Figure 4B), indicating a stronger interaction, and the corresponding broad −OH stretching band of the COOH group appears near 3000 cm^{-1}, with a shoulder extending down to 2500 cm^{-1} (Figure 4A).

In liquid cell measurements (Figure 4, C and D), where CH_3-$(CH_2)_6$−COOH was used as a model molecule for the −COOH surface, the main P═O band due to the interaction is found at 1211 cm^{-1}. The 1211 cm^{-1} peak is the dominating one in mixtures close to 1:1 but also at lower DMMP concentrations. With excess of DMMP there is also a band due to self-association showing up at ∼1247 cm^{-1}. There is a slight difference in the intensity distribution for the two main peaks

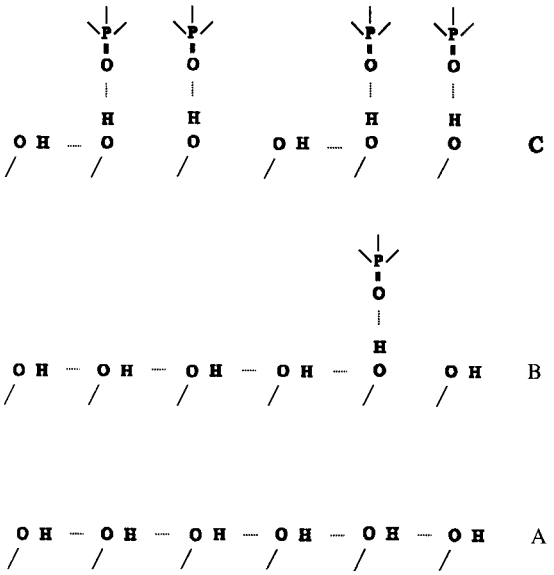

Figure 3. Schematic view of the hydrogen-bonded surface OH groups at different DMMP coverage. The figure only shows an idealized picture of one chain and the principal effect that the adsorption has on the hydrogen-bond structure. (A) shows the lateral chains of hydrogen-bonded surface hydroxyls at the undisturbed OH SAM. The transition moments of the lateral OH bonds are essentially parallel to the surface and do not appear in the spectra due to the surface selection rule.[10] The low coverage of DMMP shown in (B) allows long OH···OH chains to be present, and the P═O (1235 cm^{-1}) and OH (∼3350 cm^{-1}) bands indicate strong interaction. At high coverage (C) only short chains remain and the P═O (1242 cm^{-1}) and OH (∼3450 cm^{-1}) bands are consistent with a weaker interaction.

at ∼1210 and ∼1220 cm^{-1}, in favor for the lower position, as compared to the adsorbed DMMP (Figure 4B). This indicates that the interaction with the more free −COOH in the solution allows a higher degree of optimal hydrogen bonding than with the COOH groups anchored to the surface. However, the orientation of the molecule on the surface can also lead to the observed difference due to the surface selection rule,[10] and no definite conclusions about the origin of this relative intensity change can be drawn. Also, the broad bands due to the hydrogen-bonded OH (at ∼3000−2500 cm^{-1}) (Figure 4C) are similar to those in Figure 4A, but the strong C−H bands of the acid obscure the details. In the C−H stretch region there are a number of negative and positive peaks (Figure 4A). Two positive bands at 2960 and 3014 cm^{-1} are due to DMMP. The DMMP peak at 2859 cm^{-1} is probably obscured by the negative peak at 2861 cm^{-1}. If we compare the positions of the negative (2861 cm^{-1}) and the new positive peaks at 2918 and 2848 cm^{-1} with the bands of the used SAM, we can conclude that together they indicate a slight increase in the order of the hydrocarbon backbone of the monolayer. An increase at positions of the CH_2 absorptions characteristic for densely packed monolayers (2918 [ν_a] and 2848 cm^{-1} [ν_s]) and a decrease at the high wavenumber side of the same peaks form the argument for that. Thus, the breaking or perturbation of lateral hydrogen bonds at this surface allows the SAMs to relax and line up in a more favorable way for the hydrocarbon backbones.

Another sign of the interaction is given by the C═O of the carboxylic acid group (Figure 5A). The positions found in the monolayer 1741 and 1718 cm^{-1} have previously been assigned to free and hydrogen-bonded C═O, respectively, and calculations have shown that the terminal −COOH group is oriented, leaving the −OH group exposed toward the ambient.[17] The nature of the hydrogen bond is, however, a matter of discussion, and it has been suggested that short linear polymeric chains[17] or sideways dimeric structures are formed.[18] In any case some of the carbonyls are hydrogen bonded with a neighboring −OH, and this pattern will inevitably be affected if DMMP interacts via hydrogen bonding to that −OH group. Upon adsorption of DMMP a decrease in the hydrogen-bonded peak intensity can be seen (negative peak at 1718 cm^{-1}). At the same time a broad peak at ∼1730−1740 cm^{-1} increases, in agreement with the dissociation of lateral hydrogen bonds present on the surface. At higher DMMP coverage the peak due to free C═O at 1741 cm^{-1} decreases, probably due to interaction with the adsorbed DMMP.

A liquid cell experiment is shown in the same spectral region in Figure 5B. The pure acid as well as mixtures with small amounts of DMMP show one single peak at ∼1711 cm^{-1}, as expected for hydrogen-bonded "facing dimeric" C═O. At the 1:2 and 1:1 mixtures a band at 1726 cm^{-1} is showing up. This is a new position, rather than a combination of the known bands, and its origin is most probably C═O groups interacting with the rather polar DMMP (dipole−dipole). The interaction causes the mode frequency to shift from that of the free C═O found with excess acid (a shoulder at 1741 cm^{-1}), where the main interaction is with the nonpolar hydrocarbon chains. Compared with these results the position of the C═O band created upon adsorption of DMMP on the surface (∼1730−1740 cm^{-1}) is a combination of the free $-CH_3$ interacting 1741 and the 1726 cm^{-1} band due to dipole−dipole interacting C═O groups. Thus, the adsorption causes dissociation of lateral hydrogen bonds present on the surface, leading to new forms of interaction. The preferred adsorption on this surface can be explained by the strong hydrogen bonds formed between the acid group and the P═O group of DMMP. As in the case of the −OH surface, the formation of hydrogen bonds leads to a reorientation of the surface groups. The reorientation is also here increasing the integrated peak intensity of the OH band which nicely follows the isotherms in Figure 1.

DMMP−CH_3 Interaction. In the case of the $-CH_3$ surface no signs of interaction could be seen in the spectra even at higher DMMP concentrations. This is due to the low surface coverage found in the SAW experiments and can be explained by the expected weak interaction with this surface. Here it can also be claimed that the subtraction procedure used to compensate for gas-phase absorption in the spectra introduces a more serious error, because more molecules adsorb with the P═O part pointing out from the surface leaving them without shift. However, the gas-phase absorption needed to compensate the free P═O in the subtraction procedure showed no difference to the other surfaces, and this error is, thus, of little relevance.

An upper limit for the amount of DMMP adsorbed on this surface can be calculated by comparing the noise level at the position of the (missing) CH_3 mode at 1315 cm^{-1}, taken as the maximum peak height possibly present (spectrum not shown), with the same peak at the −OH surface. This gives a maximum coverage that is even lower than that indicated by the SAW isotherm corrected for adsorption on the naked quartz. Thus, the necessity to correct results from SAW measurements obtained with this type of weakly interacting surface is confirmed, and there might even be a need for extended corrections, taking effects other than the pure mass loading into account.

Dosing DMMP at 100 K. In a previous study the adsorption of DMMP at 100 K on the $-CH_3$ and −OH surfaces was examined with IRAS and TPD, at different coverages.[5] Here the adsorption of two doses of DMMP on a −COOH surface

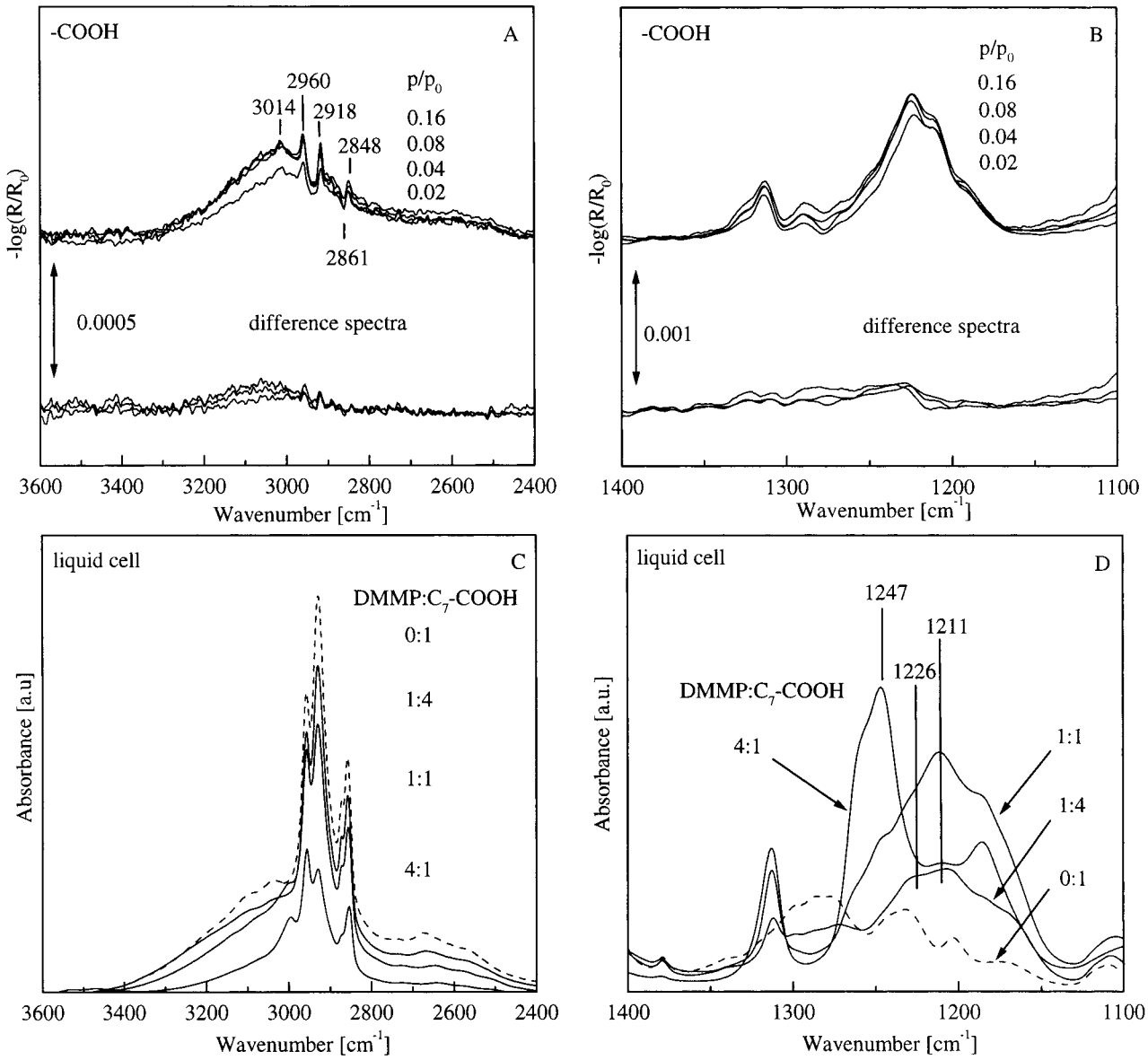

Figure 4. IRAS spectra of DMMP adsorbed on the −COOH surface shown in the high wavenumber range (A) and the low wavenumber range (B). The relative concentrations of DMMP are indicated, and the difference spectra are obtained by subtracting the $p/p_0 = 0.02$ spectrum from the higher concentration ones. Liquid cell measurements of DMMP and C_7-COOH are shown in the high wavenumber range (C) and the low wavenumber range (D), with the molar ratios indicated in the figures.

will be discussed and compared with the previous results. These UHV investigations give additional information about the type and strength of interaction(s) involved.

The spectra of DMMP deposited at 100 K on a −COOH surface show mainly the same peaks as at room temperature, and it can be concluded that even at the lowest coverage the molecules are adsorbed without dissociation on the surface. At this coverage (∼1 monolayer) the hydrogen-bonded P═O has a peak maximum at 1215 cm^{-1} and a shoulder at 1207 cm^{-1}, but there are also several bands at even lower positions (Figure 6A). A shoulder on the high wavenumber side indicates that some molecules also experience weaker interaction, probably due to self-association. Increasing the dose to 4 langmuirs (∼2 monolayers), the intensity of all bands increases, and the most pronounced change is the appearance of a peak at 1245 cm^{-1}. This is the position found to be due to multilayers in the previous study.[5] Compared to the room-temperature results discussed above, the UHV data indicate a stronger interaction at 100 K, as the hydrogen-bonded P═O peak is shifted to lower wavenumbers. There are also some changes in the carbonyl band of the SAM (Figure 5A). A positive band at 1726 cm^{-1} indicates the formation of weak C═O interaction with adsorbed DMMP, as in the case of room-temperature adsorption. However, a corresponding decrease at positions characteristic for a loss of hydrogen-bonded carbonyls (1718 cm^{-1}) is missing, and the negative band is instead found at the position of free C═O (1741 cm^{-1}). The band appearing at 1726 cm^{-1} is in good agreement with that found for a 1:1 ratio in the liquid cell results (Figure 5B), indicating that the adsorption of DMMP at 100 K does not break lateral H bonds but rather changes the environment for the C═O groups from vacuum to polar. However, as hydrogen bonding to the P═O of DMMP does occur, there must be enough free carboxylic acid −OH groups present on the surface with which the DMMP can interact.

To obtain an independent value of the strength of interaction, temperature-programmed desorption was performed. After deposition, at 100 K, the surface was heated at a constant rate of 0.33 K s^{-1}, and the desorbing molecules were monitored with a mass spectrometer. The cracking products of DMMP were determined, and we are using the strongest peak (m/e =

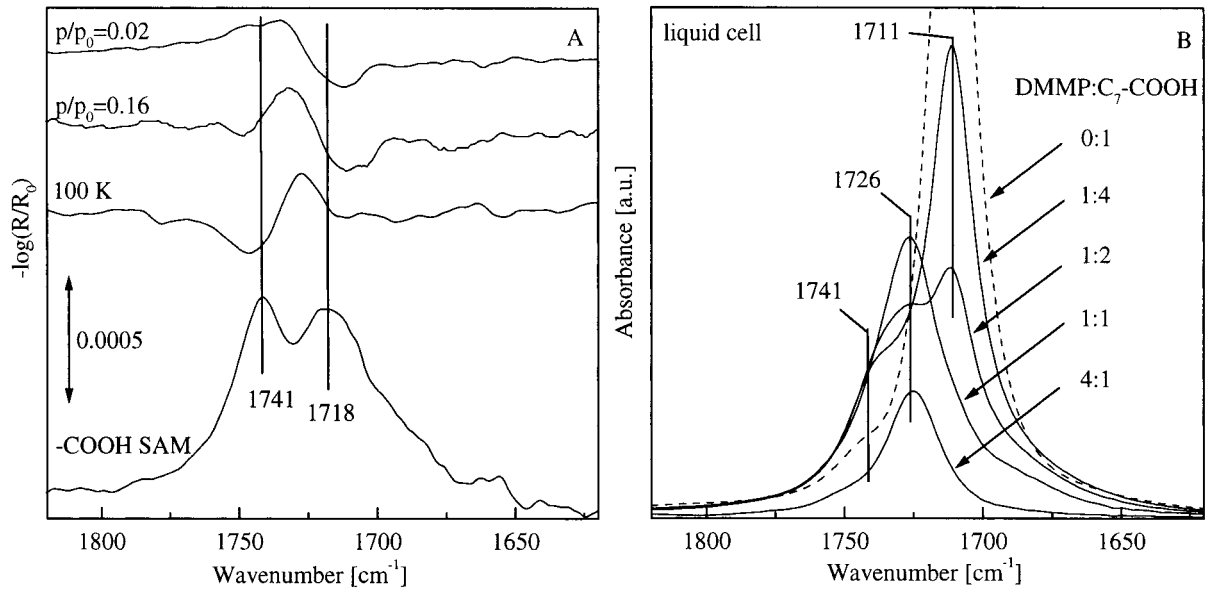

Figure 5. In (A) IRAS spectra of the C═O double peak of the −COOH SAM (bottom) and the change in these peaks upon room-temperature adsorption of DMMP at a relative concentration of 0.02 and 0.16 and DMMP adsorption at 100 K are shown. In (B) liquid cell measurements of DMMP and C_7-COOH are shown in the same wavenumber range, with the molar ratio indicated in the figure.

15, probably CH_3^+) in the analysis. There were no signs of decomposition of DMMP at the surface, and the cracking products found during desorption were the same as in a test were the masses where followed during deposition. The desorption peaks for two doses of DMMP, corresponding to 1 and 4 langmuirs, are shown in Figure 6B. Also shown in the figure are the results from the same experiment on the two other surfaces (−OH, $-CH_3$) using a dose of 1 langmuir, taken from ref 5. The low dose results in one peak at 218 K on the −COOH surface. Upon additional dosing (4 langmuirs) a peak at ∼190 K also appears, which is due to multilayers.[5] Compared to the −OH and $-CH_3$ surfaces, desorption of the monolayer dose occurs at higher temperature for this surface, indicating stronger interaction. This is in good agreement with the SAW results and also with the increasing downward shift of the P═O peak position. Thus, there seems to be a correlation between the increase in the desorption peak temperature and the gradual increase in the shift of the P═O peak, in going from the $-CH_3$ surface (1246 cm^{-1}) over the −OH surface (1228 cm^{-1}) to the −COOH surface (1215 cm^{-1}) at 100 K.[5] The broader character of the desorption peak for the −COOH surface also indicates a distribution of the adsorption energies (sites), which is in good agreement with the broad character of the P═O peak in the infrared spectrum.

The presented data give two different possibilities to quantify the strength of interaction. Comparing these two approaches, one should bear in mind that they are of different origin and different assumptions have been made in the calculations, which imply that the values obtained should not be taken absolute but rather as a convenient way to compare the surfaces. Both methods result in estimations of the strength of interaction expressed as an energy. The parameter, c, from the BET[9] curves (eq 2) contains the enthalpy of adsorption at room temperature, and the peak temperature of the TPD traces can be used to calculate a value of the activation energy of desorption at lower temperatures. The enthalpy of adsorption of the first monolayer, ΔH_a, is in the BET theory related to the enthalpy of adsorption on top of the first monolayer and on all further monolayers which is most often taken to be equal to the heat of liquefaction, ΔH_l. With the standard expression (eq 3), the c values from the curves fitted to the adsorption isotherms in Figure 1 can be used to calculate ΔH_a. With an enthalpy of liquefaction of 52.3 kJ/mol for DMMP,[19] the following values are obtained for DMMP adsorbed on the three surfaces: 57.7 kJ/mol ($-CH_3$), 60.6 kJ/mol (−OH), and 64.0 kJ/mol (−COOH). From the peak temperature of the TPD traces a value of the activation energy of desorption can be calculated using Redhead theory.[20] If a first-order desorption and a value of the preexponential factor ν of 10^{13} s^{-1} is assumed, the following values are obtained for DMMP desorbing from the three surfaces: 49.3 kJ/mol ($-CH_3$), 52.7 kJ/mol (−OH), and 59.4 kJ/mol (−COOH). Even though a direct comparison of the absolute values is nontrivial, the trend is the same for the two methods. There is an increase in the strength of interaction in going from a methyl to a hydroxyl surface of 2.9_{BET} and 3.4_{TPD} kJ/mol, respectively, and in going from the hydroxyl to the acid surface, 3.4_{BET} and 6.7_{TPD} kJ/mol, respectively. The more pronounced increase as measured with TPD in the latter case could be explained by a difference in the interaction at the two temperatures given by the different rigidity of the surface −COOH groups. This is supported by the fact that no signs of changes in the hydrocarbon backbone can be seen at 100 K (not shown) and by the difference in the change of the C═O peak, indicating that no lateral hydrogen bonds are broken at 100 K. Together with the lower P═O positions found at 100 K, our TPD data indicate that the hydrogen bonds formed with the acids increases the interaction energy to a higher extent at lower temperatures.

The energies obtained can be related to the influence on the interacting P═O part of DMMP as measured by the shift in the P═O mode (Figure 7). This visualizes the correlation between the interaction with this part of the DMMP molecule and the strength of interaction. It is possible to use the infrared data for the −OH surface presented in Table 3 to think of a possible correction for the coverage-dependent enthalpy of interaction in the BET theory. This would lead to an isotherm with higher coverage at low vapor pressure, as the P═O peak position indicates stronger interaction at low coverage. A sensor based on this interface would, if this holds, show a better response at low concentrations. A comparison with the response measured with the same device and sensing interface and an DMMP concentration of ∼0.3 ppm ($\theta \approx 2\%$)[6] shows that this correction indeed would lead to a more correct isotherm in this concentra-

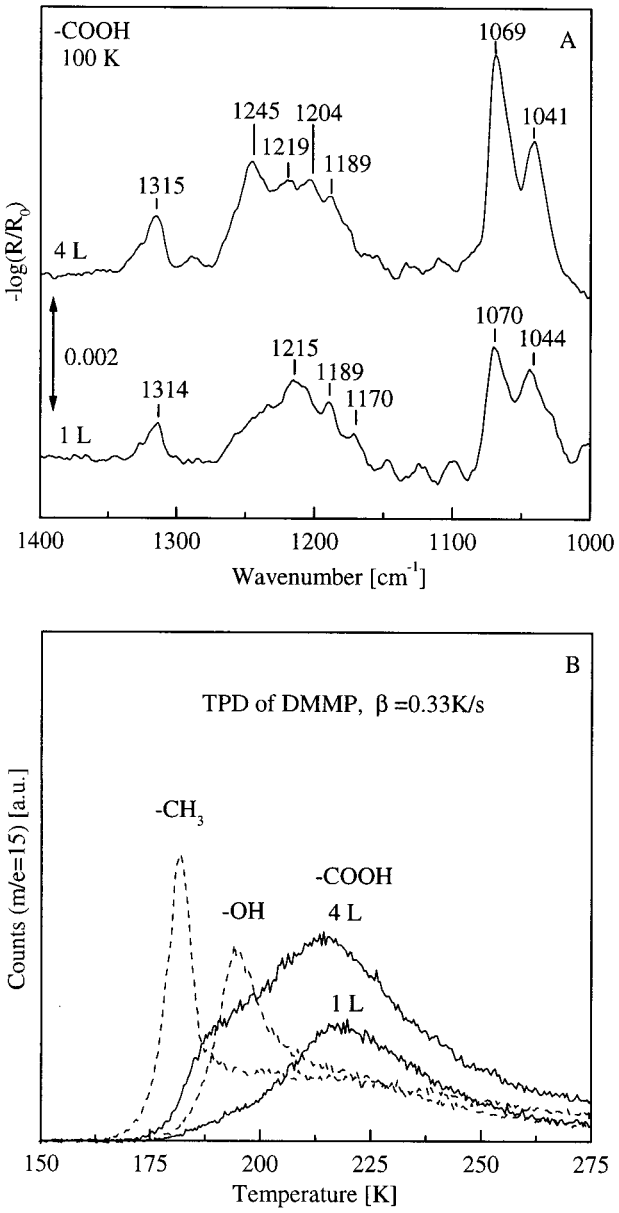

Figure 6. IRAS spectra of two different DMMP doses (1 and 4 langmuirs) adsorbed and measured at 100 K on the −COOH surface are shown in (A). In (B) the TPD traces ($m/e = 15$) of the same doses on the −COOH surface are shown, together with results from TPD of 1 langmuir doses on the $-CH_3$ and −OH surfaces (dashed lines), taken from ref 5. The traces, probably originating from CH_3^+, were recorded using a linear heating ramp of 0.33 K s^{-1}.

tion range, but the quantitative uncertainty in the correction, as well as in the measured adsorption at this low concentration, prevents any detailed conclusions to be drawn.

Comparing the increase in the enthalpy of adsorption due to hydrogen bonds with the expected enthalpy of a hydrogen bond (10−30 kJ/mol), it becomes obvious that the values obtained are smaller than expected. This difference has been observed for adsorption of D_2O on SAMs as well.[8] The discrepancy could be explained either if the hydrogen bonds formed are far from ideal or if the heat needed to break already existing lateral hydrogen bonds is considered. Hydrogen bonds have a strong bond angle dependence, and steric hindrance due to the rigidity of the used SAMs could be an explanation of nonideal hydrogen bonds. However, as the P═O peak shifts are similar to those measured in solution, this is a less probable explanation. It is, thus, more plausible that what is measured by the two methods

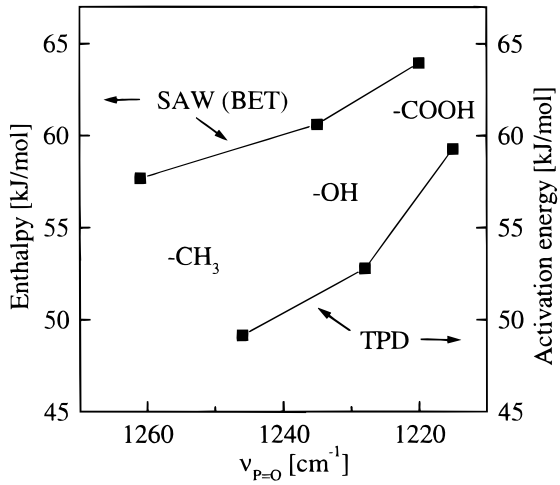

Figure 7. Two sets of data relating the shifted position of the P═O vibration to the strength of interaction between DMMP and the three surfaces indicated. The enthalpy of adsorption (left), obtained from BET fits of the SAW isotherms in Figure 1 and calculated using an enthalpy of liquefaction ($H_l = 52.3$ kJ/mol). In the TPD case the activation energy of desorption (right) was calculated using first-order Redhead[20] theory with a preexponential factor, ν, of 10^{13} s^{-1}. In this case the infrared P═O positions were measured at 100 K.

is the difference between the heat of the lateral hydrogen bonds and the heat of those formed with DMMP (Figure 3).

It can be concluded that the possibility of forming hydrogen bonds results in a relevant increase in the equilibrium adsorption at room temperature and that this could be used in the development of interfaces for sensor applications. The detailed analysis of the interaction between DMMP and the three different organic interfaces shows also that the moderate quantitative difference in the interaction involved has a pronounced influence on the adsorption.

Conclusion

There is an increased adsorption of DMMP on surfaces where possibilities to form hydrogen bonds are given. This is seen as a higher equilibrium coverage as measured by the SAW sensor and infrared absorption. The strength of interaction as calculated from BET fits of the adsorption isotherms or by the activation energy of desorption, obtained in TPD experiments, correlates with the strength of the hydrogen bonds formed with the P═O part of DMMP, as measured by shifts in the position of the P═O vibration. This vibrational mode is known to be sensitive to interactions and can thus be used as a measure of the capability of the surface to adsorb DMMP.

The strongest interaction is found for the −COOH surface where the hydrogen bonds with the adsorbed DMMP replace intermolecular lateral hydrogen bonds in the SAM, which also causes the degree of order in the hydrocarbon chains to increase slightly. For the −OH surface the interaction with DMMP is moderate at intermediate coverages, but a pronounced increase in the strength of interaction is observed at low coverages. This is explained by the presence of long chains of hydrogen bonded −OH groups, which increase the strength of the individual bonds. The CH_3 surface shows very weak interaction with DMMP, and the SAW results are found to be mainly due to adsorption on the hydrophilic parts of the SAW device not covered with the SAM.

Finally, we can conclude that the used SAMs are suitable for this type of detailed interaction study. The advantage with the SAMs is that the adsorption is governed entirely by the

nature of the tail groups used. This is proven by the absence of changes in the hydrocarbon chain conformation as measured by the positions of the C−H stretching bands upon adsorption of DMMP. In fact, a slight increase in the order of the monolayer in the case of the −COOH surface and changes in the orientation of the outermost methylene groups on the two other surfaces are the only effects registered during the adsorption experiments performed.

Acknowledgment. Part of the project was supported by the European Commission (Contract ERBCHBICT930832) and the Swedish Natural Science Research Council (Dnr. Ö-HC 10593-300) by a HCM grant and part from BWB (Contract E/B31E/I0095/G5210/). The project was also supported by a grant from the Swedish Research Council for Engineering Science (TFR). The professional assistance from Dr. Fröhlich, Dr. Jungnickel, and Dr. Enderlein (Paul Drude Institut für Festkörperphysik, Berlin) during the design and production of the SAW devices is gratefully acknowledged. We also would like to express our thanks to Prof. Lars Gunnar Ekedal for helpful discussions.

References and Notes

(1) (a) Hedge, R. I.; Greenlief, C. M.; and White, J. M. *J. Phys. Chem.* **1985**, *89*, 2886. (b) Templeton, M. K.; Weinberg, W. K. *J. Am. Chem. Soc*. **1985**, *107*, 774. (c) Henderson, M. A.; White, J. M. *J. Phys. Chem*. **1986**, *90*, 4607. (d) Hedge, R. I.; White, J. M. *Appl. Surf. Sci*. **1987**, *28*, 1. (e) Henderson, M. A.; White, J. M. *J. Am. Chem. Soc*. **1988**, *110*, 6939.

(2) (a) Porter, M. D.; Bright, T. B.; Allara, D. L.; Chidsey, C. E. D. *J. Am. Chem. Soc*. **1987**, *109*, 3559. (b) Swalen, J. D.; Allara, D. L.; Andrade, J. D.; Chandross, E. A.; Garoff, S.; Israelachvili, J.; McCarty, T. J.; Murray, R.; Pease, R. F.; Rabolt, J. F.; Wynne, K. J.; Yu, H. *Langmuir* **1987**, *3*, 932. (c) Ulman, A. *An Introduction to Ultrathin organic films From Langmuir Blodgett to Self-Assembly*; Academic Press: San Diego, CA, 1991. (d) Bertilsson, L.; Liedberg, B. *Langmuir* **1993**, *9*, 141. (e) Xu, J.; Li, H.-L. *J. Colloid Interface Sci*. **1995**, *176*, 138.

(3) Martin, S. J.; Frye, G. C.; Senturia, S. D. *Anal. Chem*. **1994**, *66*, 2201.

(4) Thomas, R. C.; Zang, H. C.; DiRubio, C. R.; Ricco, A. J.; Crooks, R. M. *Langmuir*, **1996**, *12*, 2239.

(5) Bertilsson, L.; Engquist, I.; Liedberg, B. *J. Phys. Chem. B* **1997**, 101, 6021.

(6) Bertilsson, L.; Potje-Kamloth, K.; Liess, H.-D. *Thin Solid Films* **1996**, *882*, 284.

(7) Theoretical calculation made by Dr. Fröhlich, Dr. Jungnickel, and Dr. Enderlein (Paul Drude Institut für Festkörperphysik, Berlin), private communication.

(8) Engquist, I.; Lundström, I.; Liedberg, B. *J. Phys. Chem*. **1995**, *99*, 12257.

(9) (a) Brunauer, S.; Emmett, P. H.; Teller, E. *J. Am. Chem. Soc*. **1938**, *60*, 309. (b) Steele, W. A. *The Interaction of Gases with Solid Surfaces*, Pergamon Press: Oxford, 1974.

(10) (a) Greenler, R. G. *J. Chem. Phys*. **1966**, *44*, 310. (b) Francis, S. A.; Ellison, A. H. *J. Opt. Soc. Am*. **1959**, *49*, 131.

(11) Bertilsson, L.; Liedberg, B. *Langmuir* **1993**, *9*, 141.

(12) Sprik, M.; Delamrche, E.; Michel, B.; Röthlisberger, U.; Klein, M. L.; Wolf, H.; Ringsdorf, H. *Langmuir* **1994**, *10*, 4116.

(13) Gutman V. *The Donor−Acceptor Approach to Molecular Interactions*; Plenum Press: New York, 1978.

(14) Bellamy, L. J. *The Infrared Spectra of Complex Molecules*; John Wiley & Sons: NewYork, 1975.

(15) Nuzzo, R. G.; Dubois, L. H.; Allara, D. L. *J. Am. Chem. Soc*. **1990**, *112*, 558.

(16) Atre, S. V.; Liedberg, B.; Allara, D. L. *Langmuir* **1995**, *11*, 3882.

(17) Nuzzo, R. G.; Dubois, L. H.; Allara, D. L. *J. Am. Chem. Soc*. **1987**, *109*, 3559.

(18) Smith, E. L.; Alves, C. A.; Anderegg, J. W.; Porter, M. D.; Siperko, L. M. *Langmuir* **1992**, *8*, 2707.

(19) Kosolapoff, G. M. *J. Chem. Soc*. 1954, 3222.

(20) Redhead, P. A. *Vacuum* **1962**, *12*, 203.

(21) Socrates, G. *Infrared Characteristic Group Frequencies*, John Wiley & Sons: New York, 1980.

(22) Barnes, A. J.; Lomax, S. *J. Mol. Struct*. **1983**, *99*, 137.